Available online at www.sciencedirect.com
SCIENCE DIRECT®
Journal of Sound and Vibration 291 (2006) 723–739
JOURNAL OF SOUND AND VIBRATION
www.elsevier.com/locate/jsvi

Handling uncertainties in mixed numerical-experimental techniques for vibration based material identification

T. Lauwagie[a,*], H. Sol[b], W. Heylen[a]

[a]*Department of Mechanical Engineering, Katholieke Universiteit Leuven, Celestijnenlaan 300b, B-3001 Leuven, Belgium*
[b]*Department of Mechanics of Materials and Constructions, Vrije Universiteit Brussel, Pleinlaan 2, B-1050 Brussels, Belgium*

Received 29 July 2004; received in revised form 22 June 2005; accepted 23 June 2005
Available online 2 September 2005

Abstract

Mixed numerical-experimental techniques (MNETs) combine experimental test results and numerical modelling techniques with the goal of identifying physical properties. Experimental results always come with a level of uncertainty. This input uncertainty will migrate through the MNET routine, and will result in an uncertainty on the identified parameters. Therefore, MNET procedures should not only provide an estimated value for the physical properties, they should also provide additional information about the reliability of the results obtained. This paper presents a routine that is able to transform the uncertainty on the input parameters of a MNET into the uncertainty on the output parameters. The approach does not require any change of the initial MNET routine, it is just an additional computational step that has to be performed after the MNET has identified the deterministic values of the unknown physical properties. The routine is demonstrated on a vibration based MNET used to identify elastic material properties.

1. Introduction

Vibration based material identification methods are founded on the fundamental relation between the vibratory behaviour of a structure and its elastic material properties. These methods derive the elastic material properties from the measured vibratory behaviour of a test sample. The

*Corresponding author.
E-mail address: tom.lauwagie@mech.kuleuven.be (T. Lauwagie).

0022-460X/$ - see front matter © 2005 Elsevier Ltd. All rights reserved.
doi:10.1016/j.jsv.2005.06.025

earliest identification methods based on this principle used analytical formulas to describe the vibratory behaviour of the specimens. The analytical models are restricted to homogeneous and isotropic materials, and are the limiting factors to extend the vibration based techniques to more complex materials such as orthotropic or layered materials. In 1986, Sol [1] successfully replaced the analytical formulas by special purpose finite element (FE) models. The method he proposed could identify the four engineering constants of an orthotropic material—i.e. E_1, E_2, G_{12} and ν_{12}—from the first three resonance frequencies of a plate-shaped specimen and the fundamental bending frequencies of two beam-shaped specimens. The two beams have to be oriented parallel with the two principal material directions, Fig. 1. For unidirectionally reinforced composites, one of the beams has to be cut out of the material in the direction perpendicular to the fibre direction. In some cases, this appeared to be impossible without damaging the material of the beam. Therefore the initial method was modified, to enable identification of the material properties from the first five frequencies of the test plate. A critical review of this modified procedure can be found in Ref. [2].

The use of finite element models complicates the implementation of the identification procedure. Finite element models allow the computation of the resonance frequencies of a particular structure made out of a specific material. But the finite element formulation cannot be reversed to a formulation that provides the material properties from the resonance frequencies of the structure. The material identification problem has to be solved in an inverse way. Fig. 2 displays the general solution scheme of the identification problem. The resonance frequencies of the test sample are measured by means of a modal test. These frequencies are the target output of the finite element model. The numerical frequencies of the finite element model of the test sample are computed using a set of trail values for the unknown material parameters. The numerical and experimental frequencies can now be compared, and the values of the unknown model parameters are corrected in order minimize the differences between the two frequency sets. The improved material properties are inserted in the FE-model and a new iteration cycle is started. Once the numerical and experimental frequencies match, the procedure is aborted, and the desired material properties can be found in

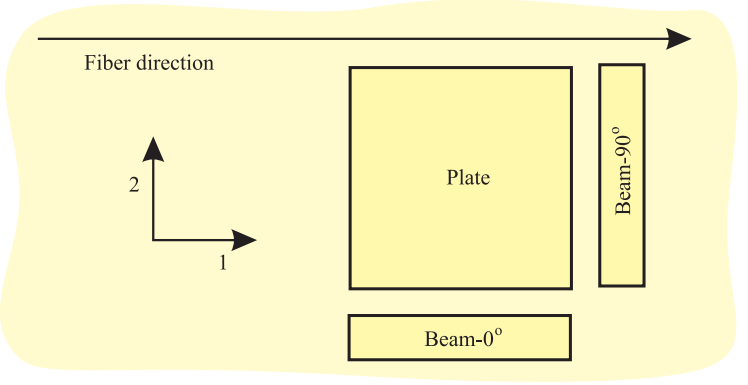

Fig. 1. Typical test specimen set for the identification method of Sol [1].

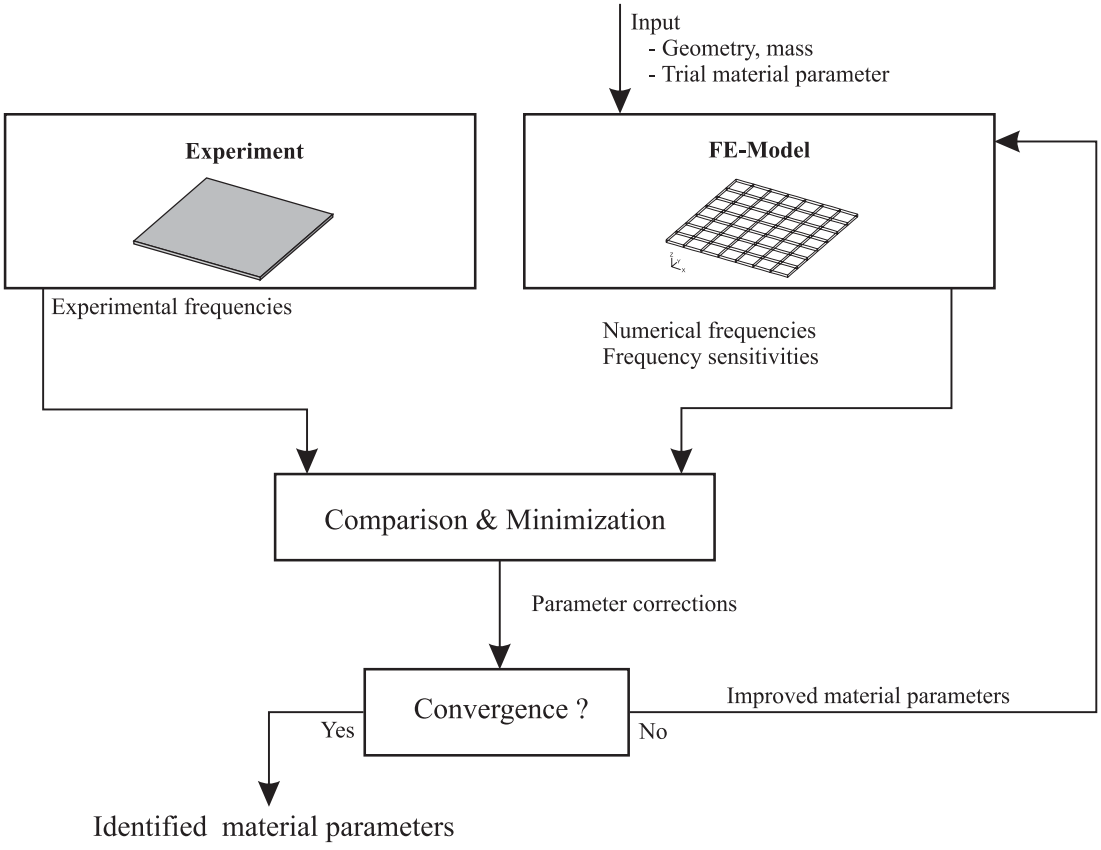

Fig. 2. General flowchart for MNET based elastic material identification procedure.

the database of the FE-model. This procedure has already proven to be a stable and reliable tool to identify elastic material properties [2].

Since these identification procedures consist of two parts, an experimental part and a numerical part, they are often referred to as mixed numerical-experimental techniques, or MNETs. Mathematically, the optimization step of the MNET can be expressed as follows [3]:

$$\underset{\Delta p}{\text{minimize}}\,(\{\Delta p\}^{\mathrm{T}}[S_m]^{\mathrm{T}}[S_m]\{\Delta p\} - 2\{\Delta r\}^{\mathrm{T}}[S_m]\{\Delta p\}). \tag{1}$$

The vectors $\{\Delta p\}$ and $\{\Delta r\}$ contain the parameter and response differences, the matrix $[S_m]$ is the sensitivity matrix and groups all the sensitivity coefficients. Each sensitivity coefficients describes the rate of change of a particular resonance frequency with respect to a changes of a specific material parameter. To ensure a stable convergence of the iterative procedure, the optimization problem (1) is solved by considering a set of box constraints on the optimization parameters—the elements of the vector $\{\Delta p\}$—in such a way that each material parameter cannot change more than 25% during one iteration step.

2. The interval approach

2.1. Measurement errors

Roughly spoken, each measurement error can be classified as one of the following types: an illegitimate error, a systematic error or a random error. Illegitimate errors are mistakes and blunders, caused by carelessness or poor judgement, i.e. misreading the display of the measurement device. Since illegitimate errors should be avoided, they will be disregarded in the rest of this text.

The second type of errors are the systematic errors. A systematic error can be defined as a reproducible error that biases the measured value in a given direction [4], i.e. a systematic overestimation or underestimation of the true value. A systematic error is by definition reproducible, therefore it cannot be reduced by taking the average value of a large number of measurements. However, the reproducible character of the systematic error makes it possible to estimate the bias on the measured value by means of a calibration procedure. The systematic error can then be compensated with the estimated value of the bias. Note that systematic errors can only be reduced by calibrating the measurement equipment, they cannot be avoided.

The last type of error is the random error. A random error causes fluctuations in the results of a measurement when the measurement is repeated a number of times [4]. Random errors occur for a variety of reasons, they can be caused by noise or other external disturbances which cannot be taken into account. Unlike systematic errors, random errors shift the measured value in an arbitrary direction. This stochastic behaviour allows to reduce random errors by averaging the values of a large number of measurements.

In the previously mentioned material identification MNETs the uncertain input parameters are the dimensions, mass and resonance frequencies of the test samples. According to our experience, the spreading on these values is almost non-existing. The uncertainty is dominated by systematic error sources like the residual offset that remains after calibration and the finite accuracy of the measurement device. The random error can therefore be ignored. The most suited way to represent these types of uncertainties are uncertainty intervals.

Note that in a MNET, the numerical models should accurately represent the considered test samples. If this is the case, the identified parameter values will be equal to the true physical values. In reality however, non-homogeneous distributions of the material properties and non-perfect constitutive relations will cause deviations between the model and reality. For the computation of the uncertainty intervals in this paper, the numerical model will be assumed to be correct, which means that only measurement errors will be considered as error sources.

2.2. Uncertainty intervals

An uncertainty interval defines an upper and lower bound between which the value of the considered parameter can vary. It does not provide any information about the probability distribution of the values between these two bounds. The following notation will be used to represent an uncertainty interval.

$$q_i \in [q_i^{(-)}, q_i^{(+)}] \quad \forall i = 1, \ldots, n_{\text{in}}, \tag{2}$$

where q_i is one of the n_{in} uncertain input parameters of the model, and can take any value which is larger than or equal to $q_i^{(-)}$ and smaller than or equal to $q_i^{(+)}$. By considering the relations between the input and output parameters f_{p_j};

$$p_j = f_{p_j}(q_1, q_2, \ldots, q_{n_{\text{in}}}) \quad \forall j = 1, \ldots, n_{\text{out}}, \tag{3}$$

the input intervals can be used to derive the uncertainty intervals on the output parameters p_j.

$$p_j \in [p_j^{(-)}, p_j^{(+)}] \quad \forall j = 1, \ldots, n_{\text{out}}. \tag{4}$$

The lower bound of this interval $p_j^{(-)}$ is the lowest possible value that can be obtained for the output parameter p_j, when all the input parameters q_i can take any value between $q_i^{(-)}$ and $q_i^{(+)}$. The upper bound $p_j^{(+)}$ represents is the highest possible value that can be obtained for the output parameter p_j. The bounds of the output intervals can be interpreted as 'worst-case' values.

2.3. Interval calculations

The most straightforward way to perform calculations with intervals is to redefine the standard mathematical operators like additions, subtractions, multiplications and divisions in such a way that they can handle intervals instead of the traditional integers or floats. This approach is generally referred to as the 'interval arithmetic' approach, and is mainly based on the work of Moore [5]. The 'interval arithmetic' approach has two major drawbacks. The first drawback deals with the practical problem of implementation. The use of the interval arithmetic concept to estimate the uncertainties on the material parameters implies that the whole identification procedure—finite-element routines, sensitivity analysis and cost function minimization—could have to be reimplemented using interval operations. The second drawback, called conservatism, is illustrated by the following example: consider a variable x that varies between 0 and 1, and calculate the interval of the variable y if $y = x^2 - x$. By ignoring the correlation between the two input parameters—x^2 and x—the result $y \in [-1, 1]$ is found. However, the correct solution to this problem is $y \in [-0.25, 0]$ and can only be obtained if the correlation between x and x^2 is taken into account. This simple example clearly indicates that ignoring existing variable correlations yields erroneous results. More details about this example, together with an extensive discussion on conservatism in interval arithmetics can be found in Ref. [6]. So far, it has not been investigated whether it is possible to keep track of the existing correlations between the variables of complex numerical procedures. With the current state of affairs, it is not possible to avoid conservatism in complex routines like finite-element solvers. Therefore, the use of interval arithmetics should not be considered to handle uncertainties in MNET based identification routines.

An alternative way to solve the interval arithmetical problem, is to reformulate it as a constrained optimization problem in which the input variables q_i are the optimization parameters, and the input–output relation is the objective function. The upper bound of the uncertainty

interval of a particular output parameter p_j can be found by maximizing the objective function, i.e. the value of the output parameter p_j, while considering the bounds of the uncertainty intervals on the input parameters as constraints on the optimization parameters—Eq. (5).

$$\begin{aligned} p_j^{(+)} \rightarrow \text{maximize} \quad & f_{p_j}(q_1,\ldots,q_{n_{\text{in}}}) \\ \text{subject to} \quad & q_i \geqslant q_i^{(-)} \quad \forall i = 1,\ldots,n_{\text{in}}, \\ & q_i \leqslant q_i^{(+)} \quad \forall i = 1,\ldots,n_{\text{in}}. \end{aligned} \tag{5}$$

The lower bound of the uncertainty interval can be found by minimizing the objective function using the same constraints on the optimization parameters. Now, consider a n_{in} dimensional space, in which each point defines a unique set of values for the different input parameters. In this input parameter space, the constraints of Eq. (5) define a n_{in}-dimensional hyper volume. Only the points inside this hyper volume are valid points, i.e. points that are associated with parameter values that comply with the considered parameter intervals. One of the commonly used approaches to solve the optimization problem (5) is to sample the hyper volume defined by the input parameter intervals, and to calculate the values of the output parameters for every sample. The highest and lowest value obtained for a particular output parameter defines the upper and lower bound of the uncertainty interval on this parameter. Fig. 3 presents a two-dimensional example. A general implementation of this approach was proposed by Hanss [7,8] and is called 'the standard method'. The procedure is applicable to a wide variety of problems but has a number of important shortcomings. The total number of samples that has to be evaluated equals $m^{n_{\text{in}}}$, where m represents the number of samples used to sample one uncertainty interval—m equals 8 in the case of Fig. 3. The total number of samples, and thus necessary computation time, increases exponentially with the number of input parameters. A second drawback is that the obtained results are only approximations of the true intervals, unless the minimum and maximum of the cost function happens to coincide with one of the sample positions. In the example of Fig. 3 the true maximum of the cost function is found, but the obtained minimum will be an approximation. The accuracy of the solution can only be improved by decreasing the sampling distance, which leads to an exponential increase of the number of samples. A small improvement

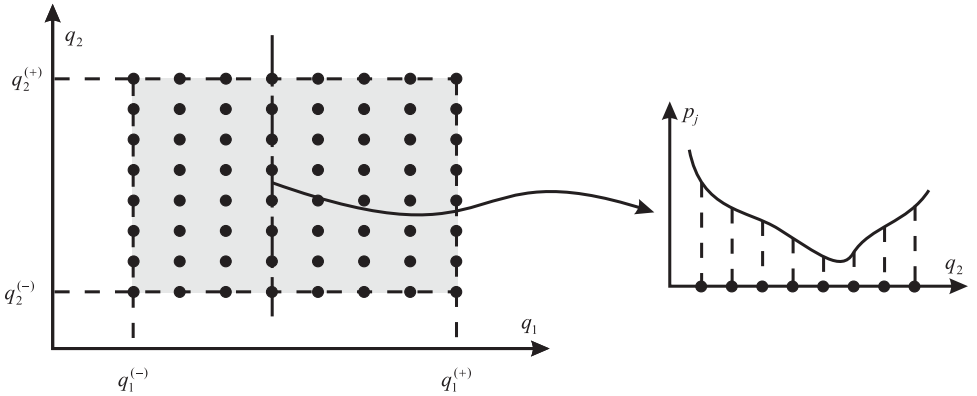

Fig. 3. Two-dimensional example of the standard method.

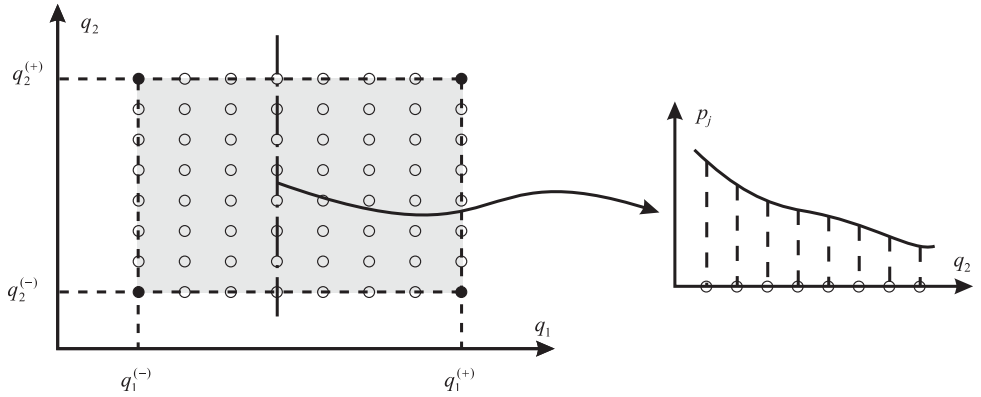

Fig. 4. Two-dimensional example of the reduced method for monotonic input–output relations.

of the accuracy will therefore be associated with a dramatic increase of the required computation time.

However, these two drawbacks are not present when the relations between the input and output parameters f_{p_j} are monotonic functions, see Fig. 4. In the case of monotonic input–output relations the extreme values of the output parameters have to lay in points where the different input parameters are maximal or minimal. This means that only the samples which are located on the vertices of the hyper volume have to be considered, all the other sample positions can be ignored since they cannot lead to an extreme value of any of the output parameters. Monotonicity of the input–output relations thus reduces the number of sample that have to be evaluated to $2^{n_{\text{in}}}$. Monotonicity also guarantees the exactness of the obtained interval bounds since the extreme values of the cost function will be reached in one of the locations of the used samples. The implementation of the standard method for monotonic input–output relations is called the reduced method.

3. The error estimation algorithm

In the case of the considered MNET identification procedures, even the application of the reduced method requires an extensive computational effort. Consider the mixed plate-beam procedure that was presented in the introduction. This routine has 17 input parameters, the application of the reduced method would require $2^{17} = 131{,}072$ runs of the identification procedure. Even with a computer platform that could run the whole identification procedure in 1 s, the uncertainty analysis would take more than 1.5 days. To reduce the computational effort, the finite element model of the identification procedure can be replaced by an approximation. An excellent approximation can be obtained by linearizing the finite element model in the working point defined by the solution of the last iteration step. The discrepancy between the initial and linearized model will be minimal because the uncertainty calculations only require tiny variations

of the model parameters. Also note that the linearization automatically ensures the monotonicity of the input–output relations.

3.1. Single-model identification routines

3.1.1. The algorithm

Linearizing the frequency response surfaces of the finite element model by computing the first-order Taylor approximation in the point defined by the obtained material parameters provides relation (6). This equation describes the influence of a variation of the material parameters on the resonance frequencies of the test specimen,

$$\{\Delta f\} = [S_m]\{\Delta p\} \tag{6}$$

in which the vector $\{\Delta p\}$ contains the applied parameter changes, the vector $\{\Delta f\}$ contains the resulting frequency changes, and $[S_m]$ is the same sensitivity matrix as in Eq. (1). The relation of Eq. (6) can be inverted by using the pseudo-inverse of the sensitivity matrix. The inversion provides Eq. (7), which expresses the influence of a change of the frequencies on the identified material parameters.

$$\{\Delta p\} = [S_m]^{\dagger}\{\Delta f\}. \tag{7}$$

Expression (7) thus allows to convert the uncertainties on the frequencies into uncertainties on the obtained material parameters. It is obvious that there is an uncertainty on the experimental frequencies, but there is also an uncertainty on the numerical frequencies. To construct the finite element model of the test specimen, the specimen's geometry and mass has to be measured. The uncertainties on the length, width, thickness and weight result in an uncertainty on the finite element model and thus in an uncertainty on the numerical frequencies. In the identification procedure the material parameters are obtained by comparing—and matching—the experimental and numerical frequencies. Therefore, the frequency uncertainties consist of two parts: an experimental part $\{\Delta f_{\text{exp}}\}$ and a numerical part $\{\Delta f_{\text{num}}\}$:

$$\{\Delta f\} = \{\Delta f_{\text{exp}}\} + \{\Delta f_{\text{num}}\}. \tag{8}$$

The uncertainties on the numerical frequencies can be related to the uncertainties on the geometrical parameters by means of a first-order Taylor approximation of the frequency response surfaces in a working point defined by the values of the geometrical parameters of the finite element model. This process results in the relation of Eq. (9).

$$\{\Delta f_{\text{num}}\} = [S_g]\{\Delta g\}. \tag{9}$$

The vector $\{\Delta g\}$ contains the geometrical parameter differences. The matrix $[S_g]$ is the geometry sensitivity matrix, and groups the partial derivatives of the resonance frequencies with respect to the length, width, thickness and mass of the sample. Inserting the expressions of Eqs. (8) and (9)

into Eq. (7) provides a relation between the uncertainties on the inputs and outputs of the identification procedure.

$$\{\Delta p\} = [S_m]^{\dagger}(\{\Delta f_{\exp}\} + [S_g]\{\Delta g\}), \tag{10}$$

$$= \underbrace{[S_m]^{\dagger}\{\Delta f_{\exp}\}}_{\substack{\textit{frequency}\\ \textit{contribution}}} + \underbrace{[S_m]^{\dagger}[S_g]\{\Delta g\}}_{\substack{\textit{geometry}\\ \textit{contribution}}}. \tag{11}$$

By grouping the terms of Eq. (11) as

$$[\chi] = [[S_m]^{\dagger} \;\; [S_m]^{\dagger}[S_g]], \tag{12}$$

$$\{\Delta\iota\} = \left\{ \begin{matrix} \{\Delta f_{\exp}\} \\ \{\Delta g\} \end{matrix} \right\}, \tag{13}$$

the influence of a change of the experimental frequencies and geometrical model parameters on a particular material property can be written as

$$\Delta p_i = \sum_j \chi_{ij}\Delta\iota_j. \tag{14}$$

To obtain the bounds of the uncertainty interval on the material property p_i, the maximum and minimum value of Δp_i have to be calculated. To maximize Δp_i, the contributions of the different summation terms $\Delta p_{i_j} = \chi_{ij}\Delta\iota_j$ have to be maximized. To express the maximum value of Δp_{i_j} in function of the input uncertainties, two different cases have to be considered. In the case where χ_{ij} is a non-negative number, the maximum contribution of the input parameter ι_j is given by

$$\max \Delta p_{i_j} = \chi_{ij}\Delta\iota_j^{(+)}, \tag{15}$$

where $\Delta\iota_j^{(+)}$ is the upper bound of the uncertainty interval on p_i. When χ_{ij} is negative, the maximum contribution to Δp_i is given by

$$\max \Delta p_{i_j} = \chi_{ij}\Delta\iota_j^{(-)} = |\chi_{ij}|\Delta\iota_j^{(+)}, \tag{16}$$

where $\Delta\iota_j^{(-)}$ is the lower bound of the uncertainty interval on p_i. The second equality of Eq. (16) is valid since the uncertainty intervals on the input parameters are assumed to be symmetrical, or $\Delta\iota_j^{(+)} = -\Delta\iota_j^{(-)}$. The combination of Eqs. (15) and (16) provides the following expression of the maximum of Δp_i.

$$\max \Delta p_i = \sum_j |\chi_{ij}|\Delta\iota_j^{(+)}. \tag{17}$$

The expression for the minimum of Δp_i can be derived in a similar way, elaboration of the problem shows that

$$\min \Delta p_i = \sum_j |\chi_{ij}|\Delta\iota_j^{(-)} = -\max\Delta p_i, \tag{18}$$

which means that the uncertainty intervals on the material properties will be symmetrical too. Also note that the relative importance of the uncertainty on a particular input parameter ι_k in the

total uncertainty on the material property p_i can be expressed as

$$\frac{|\chi_{ik}|\Delta\imath_k^{(+)}}{\sum_j |\chi_{ij}|\Delta\imath_j^{(+)}}. \tag{19}$$

Eq. (19) allows the identification of the main sources of uncertainty on a particular material parameter.

3.1.2. Example

The presented uncertainty method is illustrated using a single-plate identification routine. In this example, the material properties of a brass plate are derived from the first five plate frequencies. Table 1 presents a full description of the properties of the test plate, and the uncertainties on these properties.

The elastic material properties of the plate were identified using the deterministic values of the input parameters. The flowing results were found: $E_x = 105.0\,\text{GPa}$, $E_y = 100.0\,\text{GPa}$, $G_{xy} = 36.0\,\text{GPa}$ and $v_{xy} = 0.400$. In a second phase the uncertainty intervals on the input parameters—Table 1—were transformed into uncertainty intervals on the elastic properties using the procedure described in the previous paragraph. Table 2 presents the obtained uncertainty intervals on the identified elastic properties. Table 3 lists the relative importance of the uncertainties of the different input parameters for each output parameter.

The uncertainty on the two Young's moduli and the shear modulus is dominated by the uncertainty on the thickness. This clearly shows that an accurate measurement of the thickness is extremely important to obtain good material properties. The uncertainty on Poisson's ratio is mainly controlled by the uncertainty on the experimental frequencies. The error on the thickness and mass of the test specimen do not influence the uncertainty on Poisson's ratio. This observation can be explained as follows: the change of the thickness or the mass has the same effect on all the resonance frequencies of the test plate, which means that there is no effect on the relative difference between the frequencies. Since Poisson's ratio is not controlled by the absolute values of the frequencies but by the relative difference between the various frequencies [1], the uncertainty on the mass or thickness will not affect the uncertainty on Poisson's ratio.

Table 1
Values and uncertainties for the input parameters

	Value	Uncertainty interval			Abs. error	Units
Length	100.00	99.98	—	100.02	±0.02	mm
Width	100.00	99.98	—	100.02	±0.02	mm
Thickness	0.800	0.799	—	0.801	±0.001	mm
Mass	65.000	64.999	—	65.001	±0.001	g
Freq-1	177.20	177.11	—	177.29	±0.09	Hz
Freq-2	264.07	263.94	—	264.20	±0.13	Hz
Freq-3	353.20	353.02	—	353.37	±0.18	Hz
Freq-4	467.69	467.45	—	467.92	±0.23	Hz
Freq-5	471.66	471.42	—	471.89	±0.24	Hz

Table 2
The uncertainty intervals for the identified material properties

	Value	Uncertainty interval			Abs. error	Rel. error (%)
E_x	105.00	104.13	—	105.87	±0.8720	±0.83
E_y	100.00	99.18	—	100.82	±0.8176	±0.82
G_{xy}	36.00	35.79	—	36.21	±0.2093	±0.58
v_{xy}	0.400	0.398	—	0.402	±0.0023	±0.57

Table 3
The relative contributions of the input parameters to the output uncertainty

	Freq 1 (%)	Freq 2 (%)	Freq 3 (%)	Freq 4 (%)	Freq 5 (%)	Length (%)	Width (%)	Thick. (%)	Mass (%)
E_x	1.9	8.2	2.2	14.7	18.1	7.2	2.3	45.1	0.2
E_y	1.7	9.0	2.5	16.8	14.5	2.5	7.4	45.5	0.2
G_{xy}	11.6	2.9	2.8	5.7	5.6	3.4	3.4	64.4	0.3
v_{xy}	0.8	26.1	26.9	17.1	15.5	6.8	6.8	0.0	0.0

Table 4
Comparison between the results of the full MNET and the linear approximation

	MNET	Lin. approx.	Diff. (%)
E_x	105.8720	105.8792	0.0068
E_y	100.1443	100.1516	0.0073
G_{xy}	36.0988	36.0989	0.0004
v_{xy}	0.4010	0.4011	0.0064

3.1.3. Validation

In a first step the accuracy of the linear approximation was evaluated by calculating the worst-case scenario for the upper value of E_x with both the full MNET routine and its linear approximation. The worst-case scenario for the upper E_x value can be identified by looking at the signs of the coefficients of the first row of the χ matrix, and will be obtained with the maximal allowable values for the length, mass, the second, third and fifth resonance frequency in combination with the minimal allowable values for the width, thickness and the resonance frequencies of modes one and four. Table 4 shows the results obtained. The average error of the linearization was estimated at 0.005%. Note that this is the error for a worst-case scenario; the approximation will be even better for data points that are located closer to the working point. Because of the high accuracy and low computation time, this approximation is also very suitable for Monte Carlo simulations.

The correctness of the obtained uncertainty bounds was checked with a Monte Carlo simulation. The uncertainty intervals on the input properties were sampled using a uniform probability density distribution. In this way 5000 sets of nine input parameters—length, width, thickness, mass and five resonance frequencies—were generated. The associated material parameters were estimated with the previously validated linear approximation. Fig. 5 compares

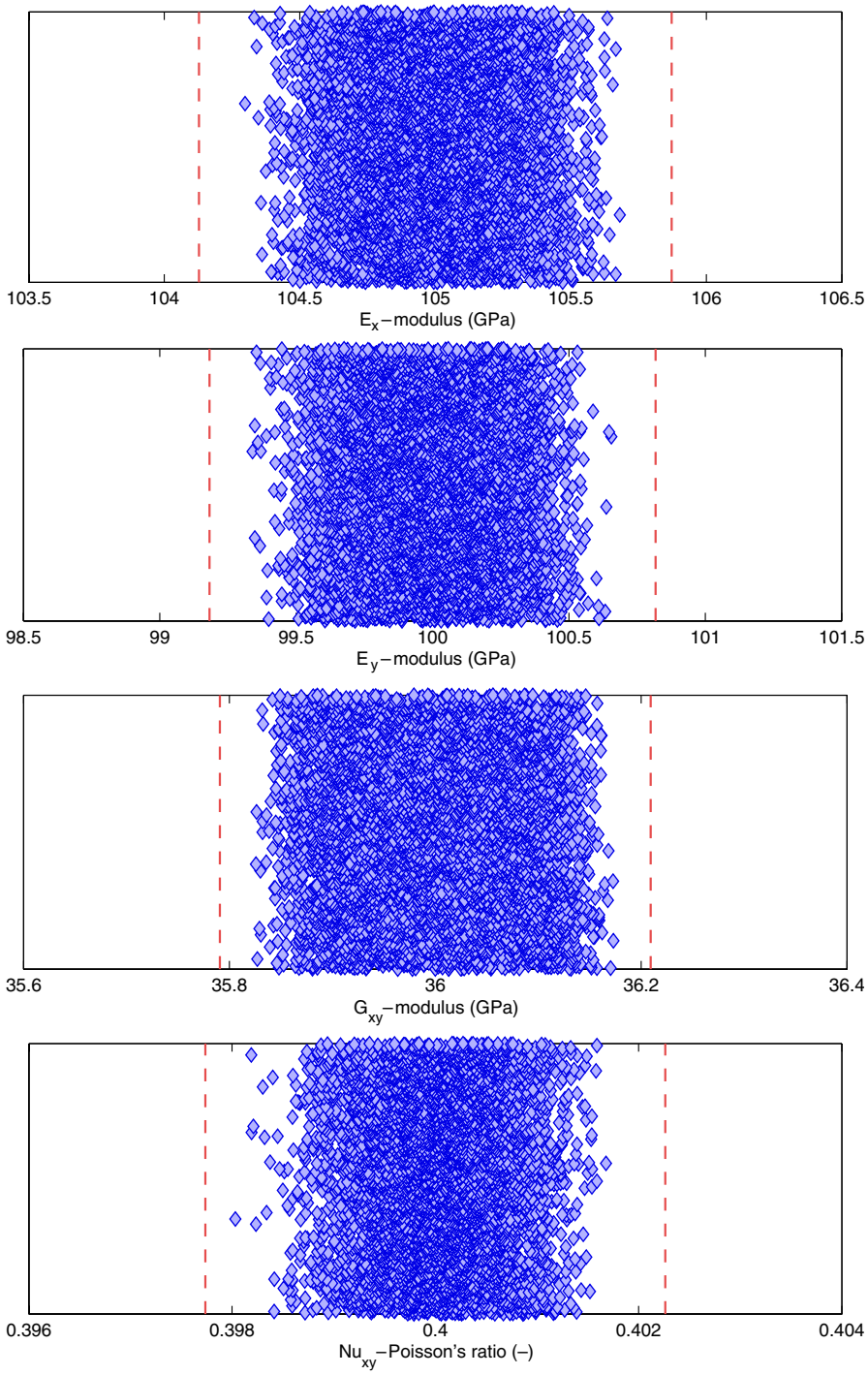

Fig. 5. The results of the Monte Carlo simulation. The dashed line represents the uncertainty bounds obtained with the presented routine.

the obtained material properties with the estimated uncertainty bounds . The most important conclusion is that none of the 5000 Monte Carlo test points results in material properties that are not contained within the predicted uncertainty bounds. Although the Monte Carlo results might give the impression that the obtained uncertainty bounds are an overestimation of the real uncertainty bounds, this is not the case. The test point that was used to evaluate the precision of the linear approximation shows that the output values on the uncertainty bound can be reached. None of the Monte Carlo test points resulted in a value close to the parameter bounds because the probability of reaching such a point is minimal—but not impossible—for a procedure with nine uncertain input parameters.

3.2. Multimodel identification routines

3.2.1. The algorithm

The method can easily be extended to handle uncertainties in multimodel identification routines. Consider a multimodel identification routine that uses resonance frequencies of n_s different test samples. The following set of equations can be written for each of the n_s models:

$$\{\Delta f^{(i)}\} = [S_m^{(i)}]\{\Delta p\} \quad \forall i \in 1, \ldots, n_s \tag{20}$$

in which the superscript $\diamond^{(i)}$ indicates that a particular quantity of the ith specimen is being considered. The equations of all the test samples can be combined to one global system as

$$\{\Delta f^{\text{glob}}\} = [S_m^{\text{glob}}]\{\Delta p\}, \tag{21}$$

where $\{\Delta f^{\text{glob}}\}$ and $[S_m^{\text{glob}}]$ are the global frequency difference vector and sensitivity matrix for the material properties, respectively. $\{\Delta f^{\text{glob}}\}$ and $[S_m^{\text{glob}}]$ are both block vectors in which the ith block line contains the data of the ith specimen, or

$$\{\Delta f^{\text{glob}}\} = \begin{Bmatrix} \{f^{(1)}\} \\ \vdots \\ \{f^{(n_s)}\} \end{Bmatrix}, \quad [S_m^{\text{glob}}] = \begin{bmatrix} [S_m^{(1)}] \\ \vdots \\ [S_m^{(n_s)}] \end{bmatrix}. \tag{22}$$

The influence of the geometrical errors on the frequencies of the finite element models of the various test specimens is given by

$$\{\Delta f_{\text{num}}^{(i)}\} = [S_g^{(i)}]\{\Delta g^{(i)}\} \quad \forall i \in 1, \ldots, n_s. \tag{23}$$

These n_s sets of equations can also be combined into one global set as

$$\{\Delta f_{\text{num}}^{\text{glob}}\} = [S_g^{\text{glob}}]\{\Delta g^{\text{glob}}\}, \tag{24}$$

where the global difference vectors are given by

$$\{\Delta f_{\text{num}}^{\text{glob}}\} = \begin{Bmatrix} \{f_{\text{num}}^{(1)}\} \\ \vdots \\ \{f_{\text{num}}^{(n_s)}\} \end{Bmatrix}, \quad \{\Delta g^{\text{glob}}\} = \begin{Bmatrix} \{g^{(1)}\} \\ \vdots \\ \{g^{(n_s)}\} \end{Bmatrix}. \tag{25}$$

The global sensitivity matrix for the geometrical parameters is a block diagonal matrix with the following structure:

$$[S_g^{\text{glob}}] = \begin{bmatrix} [S_g^{(1)}] & \cdots & [0] \\ \vdots & \ddots & \vdots \\ [0] & \cdots & [S_g^{(n_s)}] \end{bmatrix}. \tag{26}$$

In a similar way as in the single-model case, it can be shown that the maximal change of a particular material parameter can be expressed as

$$\max \Delta p_i = \sum_j |\chi_{ij}| \Delta \imath_j^{(+)} = -\min \Delta p_i, \tag{27}$$

where $[\chi_{ij}]$ and $\{\Delta \imath\}$ have the same structure as specified by Eqs. (12) and (13), but have to be calculated using the global vectors and matrices as defined by Eqs. (22), (25) and (26). Remember that Eq. (27) is only valid if the uncertainly intervals of all the input parameters—experimental frequencies and geometrical properties—are symmetrical. As in the case of a single-model identification routine, the relative importance of each input parameter in the total uncertainty on a particular material parameter can be obtained with Eq. (19).

Table 5
Values and uncertainties for the input parameters

	Value	Uncertainty interval			Abs. Error	Units
Plate						
Length	100.00	99.98	—	100.02	±0.02	mm
Width	100.00	99.98	—	100.02	±0.02	mm
Thickness	0.800	0.799	—	0.801	±0.001	mm
Mass	65.000	64.999	—	65.001	±0.001	g
Freq-1	177.20	177.11	—	177.29	±0.09	Hz
Freq-2	264.07	263.94	—	264.20	±0.13	Hz
Freq-3	353.20	353.02	—	353.37	±0.18	Hz
Beam 0°						
Length	100.00	99.98	—	100.02	±0.02	mm
Width	20.00	19.98	—	20.02	±0.02	mm
Thickness	0.800	0.799	—	0.801	±0.001	mm
Mass	13.000	12.999	—	13.001	±0.001	g
Freq-1	296.80	196.64	—	296.94	±0.15	Hz
Beam 90°						
Length	100.00	99.98	—	100.02	±0.02	mm
Width	20.00	19.98	—	20.02	±0.02	mm
Thickness	0.800	0.799	—	0.801	±0.001	mm
Mass	13.000	12.999	—	13.001	±0.001	g
Freq-1	289.61	189.47	—	289.76	±0.14	Hz

Table 6
The uncertainty intervals for the identified material properties

	Value	Uncertainty interval			Abs. error	Rel. error (%)
E_x	105.00	104.07	—	105.93	±0.9264	±0.88
E_y	100.00	99.12	—	100.88	±0.8844	±0.88
G_{xy}	36.00	35.80	—	36.20	±0.1963	±0.55
v_{xy}	0.400	0.396	—	0.404	±0.0039	±0.99

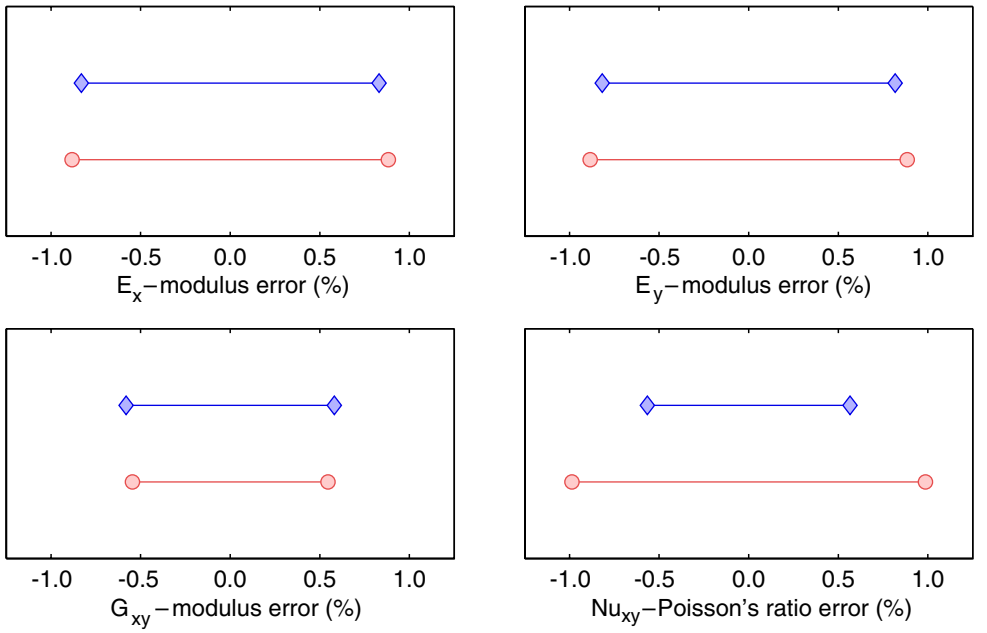

Fig. 6. Comparison of the output uncertainty of the single-plate and mixed plate-beam routines.

3.2.2. Example

The multimodel routine can estimate the uncertainty intervals on the material parameters when the mixed plate-beam identification routine is used. The uncertainty intervals on the input parameters are chosen in the same way as for the single-plate identification routine. Table 5 gives an overview of the input uncertainties, the associated output uncertainties are presented in Table 6.

The proposed uncertainty methods can be used to compare different possible test configurations. From a deterministic point of view, there is absolutely no difference between the single-plate and the mixed plate-beam identification routine, both methods yield exactly the same material properties. However, the two approaches do not result in the same uncertainty on the identified parameters—see plots of Fig. 6. There is hardly any difference between the two methods when it comes to the reliability of the identified elastic and shear modulus values, but the single plate routine results in a considerably lower uncertainty on Poisson's ratio than the mixed plate-beam routine. This indicates that the single plate routine should be preferred, especially when the goal is to estimate the value of Poisson's ratio.

3.2.3. Possibility versus probability

The multimodel algorithm also provides a opportunity to illustrate the interpretation of the uncertainty intervals. In Section 3.1.3 the uncertainty intervals were compared with the results of a Monte Carlo simulation for the case where the elastic properties were estimated from the first five resonance frequencies of one single test plate. When more test plates are available, the material properties could be estimated from the resonance frequencies of all plates by means of the multimodel updating routine. The calculation was performed for the case where two or three test plates are available. The dashed lines in Fig. 7 represent the obtained uncertainty intervals. The uncertainty intervals are the same for all three cases. It is important to know that a dramatic increase of the number of uncertain input parameters—from nine in the case of the single-plate routine to 27 in the case of the multimodel routine that uses three plates—does not automatically results in an increase of the uncertainty intervals on the identified material parameters. If the number of input parameters increases, each input parameter will have—relatively spoken—a smaller impact on the output values. This results in a smaller contribution of each input uncertainty to the output uncertainty, but the total output uncertainty will remain the same since there are more input uncertainties that are contributing.

The Monte Carlo simulations show a completely different picture, they suggest a reduction of the uncertainty. With an increasing number of input parameters, it becomes more and more unlikely that all the input parameters will shift the value of a particular output quantity in the same direction. The chance that the influence of one input parameter will be compensated by the

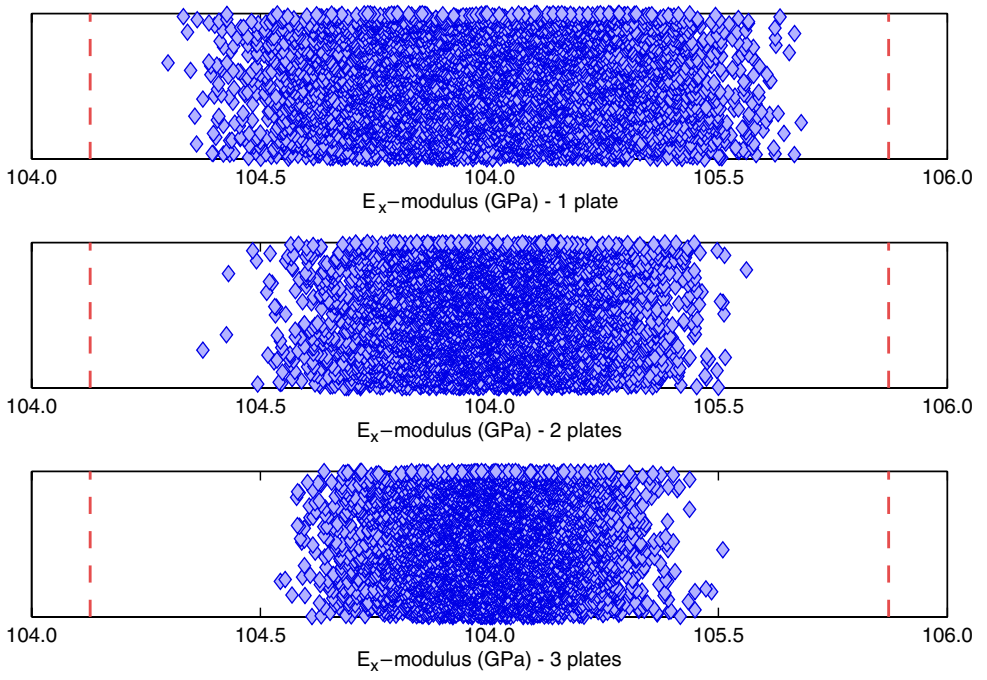

Fig. 7. Comparison between the uncertainty bounds and the Monte Carlo results for the multi-plate routines. The dashed line represents the uncertainty bounds as obtained with the presented routine.

opposite influence of another parameter increases, which reduces the probability of obtaining one of the worst-case solutions. But these worst-case values can still be obtained.

To summarize, the uncertainty intervals provide information about whether it is *possible* to obtaining a certain solution, not whether it is *probable*.

4. Conclusions

This paper introduces and validates a computationally efficient routine to handle uncertainties in MNET based material identification routines. The routine uses a linear approximation of the FE-model used in the numerical part of the MNET. It allows the calculation of the uncertainty intervals on the identified parameters from the uncertainty intervals of the input parameters and the determination of the relative importance of the various input uncertainties in the total output uncertainty. The routine also allows the comparison of two different MNET configurations based on the reliability of the results, or the identification of the main source of uncertainty of one particular MNET configuration.

The presented approach is not restricted to vibration based MNETs used to identify elastic material parameters. The approach is completely generic, and can be applied to any MNET routine of which the numerical model can be approximated with a linearized response surface in the vicinity of the working point. The quality of the obtained results will of course depend on the accuracy of the linear approximation of the model.

Acknowledgements

This work was performed in the framework of the GRAMATIC research project supported by the Flemish Institute for the Promotion of Scientific and Technological Research in Industry IWT.

References

[1] H. Sol, Identification of Anisotropic Plate Rigidities Using Free Vibration Data, PhD Thesis, Vrije Universiteit Brussel, Belgium, 1986.

[2] T. Lauwagie, H. Sol, G. Roebben, W. Heylen, Y. Shi, O. Van Der Biest, Mixed numerical-experimental identification of elastic properties of orthotropic metal plates, *NDT & E International* 36 (7) (2003) 487–495.

[3] T. Lauwagie, W. Heylen, H. Sol, G. Roebben, Determination of the in-plane elastic properties of the different layers of laminated plates by means of vibration testing and model updating, *Journal of Sound and Vibration* 274 (3–5) (2004) 529–546.

[4] National Institute of Standards and Technology (NIST). *Essentials of expressing measurement uncertainty*. http://physics.nist.gov/cuu/Uncertainty/index.html.

[5] R. Moore, *Interval Analysis*, Prentice-Hall, Englewood Cliffs, 1966.

[6] D. Moens, A Non-Probabilistic Finite Element Approach for Structural Dynamic Analysis with Uncertain Parameters, PhD Thesis, Katholieke Universiteit Leuven, 2002.

[7] M. Hanss, The transformation method for the simulation and analysis of systems with uncertain parameters, *Fuzzy Sets and Systems* (2002).

[8] M. Hanss, S. Oexl, L. Gaul, Simulation and analysis of structural joint models with uncertainties, in: *Proceedings of the Structural Dynamics Modeling Conference*, Madeira, Portugal, 2002.